

Dependence of the Liquid Absorption Behavior of Nonwovens on their Material and Structural Characteristics: Modeling and Experiments

Dipayan Das,¹ Arun Kumar Pradhan,¹ Behnam Pourdeyhimi²

¹Department of Textile Technology, Indian Institute of Technology Delhi, Hauz Khas, New Delhi 110016, India

²The Nonwovens Institute, North Carolina State University, Raleigh, North Carolina 27695

Received 23 August 2011; accepted 5 December 2011

DOI 10.1002/app.36635

Published online in Wiley Online Library (wileyonlinelibrary.com).

ABSTRACT: Nonwovens are widely used as liquid absorbent products. Baby diapers, sanitary napkins, adult incontinence pads, oil sorbents, wet wipes, and wound dressings, to name a few, are excellent examples of the use of nonwovens as absorbent media. The performance of nonwoven absorbent media is determined by its liquid absorption behavior, which is characterized by the capacity of absorption and the rate of absorption. In this article, we report on the effects of the physical characteristics of the constituent fibers and the internal structure of the nonwovens on their liquid absorption behavior. A theoretical model of liquid absorption behavior of nonwovens was developed, and this model was verified with a set of experimental results obtained on real nonwoven materials.

The nonwoven materials were prepared with polyester fibers with different cross-sectional sizes and their liquid absorption properties were measured with the gravimetric absorbency testing system. We observed that the size of fiber cross sections and the porosity of the nonwovens played very important roles in determining their absorbent capacity and rate of absorption. The results of the experiments were discussed in light of the theoretical model. The theoretical results were found to be in good agreement with the experimental results. © 2012 Wiley Periodicals, Inc. *J Appl Polym Sci* 000: 000–000, 2012

Key words: absorption; fibers; modeling; nonwoven; structure

INTRODUCTION

Nonwoven materials stand out as a unique example of fibrous porous materials. They are widely used as liquid absorbent products. Baby diapers, sanitary napkins, adult incontinent pads, oil sorbents, wet wipes, and wound dressings, to name a few, are excellent examples of the use of nonwovens as absorbent media. The performance of nonwoven absorbent media is determined by its liquid absorption behavior, which is generally characterized by the liquid absorption capacity and rate of liquid absorption. Both of these characteristics are equally important to characterize the liquid absorption behavior of nonwoven absorbent media. While the liquid absorption capacity denotes about the amount of liquid absorbed by the nonwoven materials, the rate of absorbency indicates how quickly a liquid is absorbed by the nonwoven materials.

The liquid absorption behavior of nonwoven absorbent media is primarily dictated by the phenomena of wetting and wicking. Wetting is the prerequisite to wicking, and it is the first response of the fiber

aggregate system to the liquid system, whereby the fiber–air interfacial layer is replaced by the fiber–liquid interfacial layer.^{1,2} On the other hand, wicking is the spontaneous flow of liquid through the capillary, driven by the pressure difference within the capillary.² Through wicking, the liquid is transmitted in the in-plane direction and in the cross-plane direction. Wicking depends on the wetting behavior of the nonwoven absorbent media, the pore geometry of the media and the characteristics of the liquid used.^{3–6}

Numerous research studies have been conducted so far on the liquid absorbency behavior of nonwoven absorbent media. A large body of information is available on the material–process–structure–property relationships of nonwoven absorbent media that determine their liquid absorption behavior.⁷ It is known that fibers are the building blocks of nonwoven absorbent media and that their physical and chemical properties are important with respect to their liquid absorption behavior. So far, the physical properties of the fibers are concerned, the size and shape of fiber cross section play a very important role in determining the flow of liquid through the aggregate of fibers in the media.⁸ As far as the chemical properties of fibers are concerned, the polar groups present in fibers and the chemicals used for finishing determine the wetting and wicking behaviors of the nonwovens.⁷ Synthetic fibers, such

Correspondence to: D. Das (dipayan@textile.iitd.ac.in).

as polyester and polypropylene, are seen to be widely used as absorbent media. However, these fibers are hydrophobic in nature. To improve the water absorption capacity, these fibers are generally blended with cellulosic fibers or finished with hydrophilic chemicals.^{8,9} It has been reported that polyester fibers can be split to produce microfibers, and the microfibers produced this way show an excellent liquid absorption capacity.¹⁰ In one study,¹¹ it was found out that a blend of polyester and polypropylene fibers showed higher absorption capacity than a nonwoven prepared by 100% polyester fibers. However, in an another research study, it was observed that fiber blending did not affect the absorption capacity.¹² Interestingly, the effect of fiber size on the liquid absorbency behavior were observed to be different by different researchers. In one study,¹³ it was observed that coarser fibers resulted in higher absorption capacity and higher rate of absorption. However, in another research work,¹⁴ it was found that finer fibers resulted in higher absorption capacity and higher rate of absorption. The liquid absorption properties of blended nonwovens were also studied by the mixture of two fibers having different diameters.¹¹ It was reported that blending improved the liquid retention properties, but the rate of liquid absorption was the same as that of the coarser fiber. Further, it was reported that the modified deeply grooved fiber cross sections enhanced the absorption capacity and rate of absorption to a remarkable extent.¹³ If a liquid does not move over a smooth surface, it can spread through the grooved surface of the same material.¹⁴ The geometry of the groove determines the flow behavior of the liquid into and through the media.¹⁵ Apart from the fiber properties, the liquid characteristics have also been found to be important. The density, viscosity, and surface tension of the liquid are known to play important roles in determining the liquid absorption behavior. Furthermore, the structure of nonwoven materials also plays a very important role in determining their liquid absorption behavior. The liquid is mainly absorbed into the interstices of the constituent materials when the fibers are hydrophobic in nature. This type of absorption is known as *capillary sorption*. Here, the liquid does not penetrate inside the polymeric chains of the constituent fibers.¹⁶ Then, the absorption behavior of the fibrous porous media depends on the porosity and the cross-sectional size and shape of the capillaries, which, in turn, depend on the cross-sectional size, shape, and aggregate pattern of the fibers.^{7-9,17,18} Depending on the fiber size, shape, and alignment in the media, the capillaries presents in the structure may or may not be interconnected.⁵ The movement of the liquid can cause the fibers to move from their initial place and

result in a change in the mean pore size and the distribution of pore size.¹⁹

In this article, we report on the effects of the physical characteristics of constituent fibers and the internal structure of nonwovens on their liquid absorption behavior. A theoretical model of liquid absorption behavior of nonwovens was developed, and this model was verified with a set of experimental results obtained on real nonwoven materials. The experimental results are discussed in light of the theoretical model.

THEORETICAL

We considered a nonwoven material of weight W , cross-sectional area A , and thickness T . The weight per unit area (λ ; basis weight) of this material is $\lambda = W/A$ and its volume (V) is expressed by $V = AT$. The density (ρ ; mass per unit volume) of this material is defined as $\rho = W/AT$. If this density is divided by the density of the fiber (ρ_f), the packing density of the nonwoven material (μ) is obtained as follows:

$$\mu = \frac{\rho}{\rho_f}$$

Suppose that a nonwoven material consists of a number of fibers, each with a weight, length (l_f), and volume (v_f). The cross-sectional area of a fiber (a_f) is given by $a_f = v_f/l_f$. We assume that this cross-sectional area is same as that of a circle of diameter d_f , such that $d_f = \sqrt{4a_f/\pi}$. Then, d_f is called equivalent fiber diameter. The perimeter of a fiber (p_f) is given by $p_f = \pi d_f(1 + e_f)$, where e_f is known as fiber shape factor. Note that for a circular fiber, the value of e_f is equal to zero. As the shape of a fiber cross section deviates from circularity, the value of e_f increases. The surface area of a fiber (s_f) is usually expressed by $s_f = p_f l_f = \pi d_f(1 + e_f)l_f$. Then, the specific surface area of a fiber (ζ_f) is expressed as $\zeta_f = s_f/v_f = 4(1 + e_f)/d_f$.

Besides fibers, the nonwoven material contains many void spaces bound by fiber surfaces. As shown in Figure 1, the black void spaces are bound by white fibers. Let us call these void spaces *pores*. It is assumed that there are a number of pores (n_p) in the fabric. Each pore has a cross-sectional area (a_p). If the cross-sectional area of a pore is equal to that of a circle of diameter d_p such that $d_p = \sqrt{4a_p/\pi}$, d_p is called *equivalent pore diameter*. With this term, we understand the pore size. Besides the size of a pore, the cross-sectional shape of a pore is another characteristic of pore structure. This is characterized by pore shape factor (e_p), which is expressed as follows:

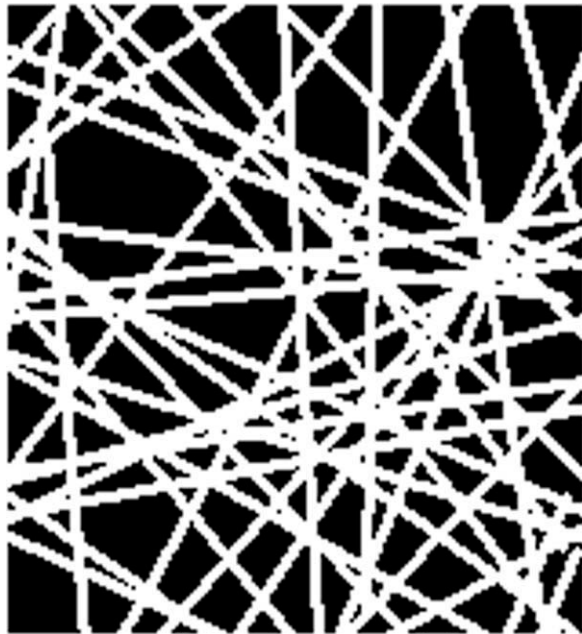


Figure 1 Schematic diagram of nonwoven structure.

$e_p = p_p/(\pi d_p) - 1$, where p_p is the perimeter of a pore. If l_p is the length of a pore, the pore surface area (s_p) can be expressed by $s_p = p_p l_p = \pi d_p(1 + e_p)l_p$. If v_p is the volume of a pore, its specific surface area (ζ_p) can be written as $\zeta_p = s_p/v_p = 4(1 + e_p)/d_p$.

It can be understood from the aforesaid discussions that the volume of the fabric (V) can be written as $V = V_f + V_p$, where V_f is the volume occupied by all of the fibers in the nonwoven and V_p is the volume occupied by all pores in the nonwoven. The ratio of the total fiber volume to the fabric volume is expressed by V_f/V , and we assign a variable (μ) to this ratio such that $\mu = V_f/V$, where $\mu \in (0,1)$ is called packing density of the nonwoven. The relative volume of pores in the nonwoven is expressed by V_p/V , and we assign a variable (ψ) to this ratio such that $\psi = V_p/V$, where ψ is called porosity of the nonwoven. Evidently, the variables ψ and μ are mutually related by $\psi = 1 - \mu$.

We assume that the total surface area of all of the pores (S_p) is equal to the sum of the surface area values of all of the fibers in the nonwoven. Then, it is possible to derive that

$$d_p = \frac{(1 + e_p) 1 - \mu}{(1 + e_f) \mu} d_f \tag{1}$$

It can be observed from eq. (1) that d_p is a function of the fiber diameter, fiber shape, pore shape, and packing density. Often, the pore shape is difficult to determine practically. It is then necessary to express the pore shape in terms of measurable quantities that determine it. To find this theoretically, the geometry of pores is often hypothesized.²⁰ One such hypothesis leads to pores with a constant e_p , that is, $1 + e_p = k$, where k is a constant. Substituting this in eq. (1), we obtain an expression for d_p in the following form:

$$d_p = \frac{k}{(1 + e_f)} \frac{1 - \mu}{\mu} d_f \tag{2}$$

Another hypothesis is related to pores with constant l_p values. Under this hypothesis, d_p takes the following form:

$$d_p = \frac{k}{(1 + e_f)} \sqrt{\frac{1 - \mu}{\mu}} d_f \tag{3}$$

It is then possible to state the following generalized expression for d_p :

$$d_p = \frac{k}{(1 + e_f)} \left(\frac{1 - \mu}{\mu}\right)^m d_f \tag{4}$$

where k and m are two constants for a nonwoven material, and they are required to be determined empirically in relation to a particular physical process, for example, liquid absorption with reference to this study.

It is well known that the absorbency is governed by a capillary phenomenon (wicking). This is illustrated in Figure 2, where γ_{fl} is the surface tension between fiber and liquid, γ_{fa} is the surface tension between fiber and air, and γ_{al} is the surface tension between air and liquid. The liquid is advancing according to the relation $\gamma_{fa} - \gamma_{fl} = \gamma_{al} \cos \vartheta$, where ϑ is the angle of contact between fiber and liquid–air interface. The values of these surface tensions and the contact angle are constant for the three given media. Obviously, the difference in the surface tensions ($\gamma_{fa} - \gamma_{fl}$) acts on the entire perimeter of the capillary (pore). The force that lifts the column of fluid is equal to $\pi d_p(1 + e_p)\gamma_{al} \cos \vartheta$, and the weight of the lifted liquid column is $(\pi d_p^2/4)h\rho_l g$, where h is the wicking height, ρ_l is the density of the liquid, and g is the acceleration due to gravity. Under equilibrium, the force that lifts the column of fluid is equal to the weight of the lifted liquid column. On



Figure 2 Scheme of wicking.

the basis of this equality and with eq. (4), it is possible to derive the following expression for h :

$$h = \frac{4\gamma_{al} \cos \vartheta}{\rho_l g} \frac{1 + e_f}{kd_f} \left(\frac{\mu}{1 - \mu} \right)^m \quad (5)$$

In this case, the parameters k and m need to be determined experimentally. The volume of liquid (V_l) wicked in a pore of d_p at h is $V_l = \pi d_p^2 h / 4$. Let us assume that there are n_p number of pores each of diameter d_p in the nonwoven. Then, n_p is determined by the ratio of the total porous area in the nonwoven to the area occupied by one pore, as expressed by $n_p = A(1 - \mu) / (\pi d_p^2 / 4)$. If all of the pores wick the liquid at h , the total volume of liquid ($V_T = n_p V_l$) wicked by all pores present in the nonwoven takes the following expression:

$$V_T = \frac{4\gamma_{al} \cos \vartheta}{\rho_l g} \frac{1 + e_f}{kd_f} A \mu^m (1 - \mu)^{1-m} \quad (6)$$

The total weight of the liquid absorbed by the nonwoven (W_T) can be calculated as $W_T = V_T \rho_l$. The total weight of the material (W) can be calculated as $W = AT\mu\rho_f$. Then, the total weight of the liquid absorbed per unit weight of the material [total absorption capacity (ξ)] can be expressed as follows:

$$\xi = \frac{W_T}{W} = \frac{4\gamma_{al} \cos \vartheta}{g} \frac{1 + e_f}{k} \frac{1}{d_f \rho_f} \frac{1}{T} \left(\frac{1 - \mu}{\mu} \right)^{1-m} \quad (7)$$

The same equation can be expressed in terms of dimensions of the variables as follows:

$$\xi_{[L]} = 4000 \frac{\gamma_{al}[\text{N/m}] \cos \vartheta_{[\text{rad}]}}{g_{[\text{m/s}^2]}} \frac{1}{k_{[1]} d_{f[\text{mm}]} \rho_{f[\text{kg/m}^3]}} \frac{1 + e_{f[1]}}{T_{[\text{m}]}} \left(\frac{1 - \mu_{[1]}}{\mu_{[1]}} \right)^{1-m_{[1]}} \quad (8)$$

Here, the dimensionless parameters k and m need to be determined experimentally. The behavior of this equation can be understood from the following example.

Suppose that a set of nonwoven materials is made up of round polyester fibers of three different diameters, 0.010, 0.020, and 0.030 mm, each at five different packing density values, 0.01, 0.05, 0.10, 0.15, and 0.20. These materials are produced in such a way that all of them have the same thickness of 20 mm. The 15 nonwoven materials thus produced are tested for their water absorption behavior. The parameters k and m are determined as follows: $k_{[1]} = 100$ and $m_{[1]} = 0.50$ for the structures made up of fibers 0.030 mm in diameter, $k_{[1]} = 50$ and $m_{[1]} = 0.70$ for the structures made up of fibers 0.020 mm in diameter, and $k_{[1]} = 25$ and $m_{[1]} =$

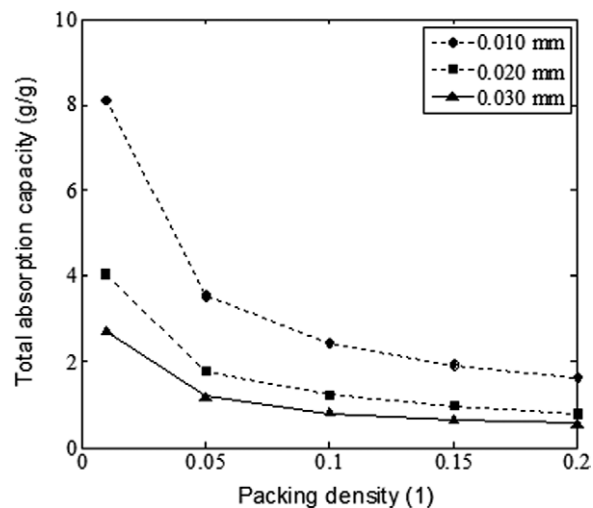


Figure 3 Plot of the total absorbent capacity against μ for different fiber diameters.

0.90 for the structures made up of fibers 0.020 mm in diameter. The surface tension between air and water is taken as 0.072 N/mm, and the angle of contact between the fiber and water is considered to be 40° . The density of the polyester fiber is taken to be 1380 kg/m³. By substituting all of these values into eq. (8), one can determine the total absorption capacity of the 15 materials, as shown in Figure 3. It can be seen that as μ increases, the total absorption capacity decreases. Also, it can be seen that as the fiber diameter decreases, the total absorption capacity increases.

EXPERIMENTAL

Fibers

In this study, round (circular) polyester fibers of three different linear densities, namely, 1.5 denier (0.17 tex), 6 denier (0.67 tex), and 15 denier (1.7 tex), were used. The cut length of all of the fibers was 51 mm. The diameters of the round fibers with linear densities of 1.5, 6, and 15 denier were found to be 0.0124, 0.0248, and 0.0392 mm, respectively. The surface areas of the round fibers with linear densities of 1.5, 6, and 15 denier were found to be 1.99, 3.97, and 6.28 mm², respectively.

Preparation of nonwoven materials

A series of nonwoven materials were prepared with 100% round polyester fibers of different linear densities and by variation of the basis weight and thickness of the materials. The details of these materials are displayed in Table I. To prepare all of these materials, the fibers were first opened with opening machines and then carded by a roller carding machine. The carded webs were then crosslapped and finally bonded with a needle-punching machine.

TABLE I
Specifications of Nonwoven Materials Prepared for this Study

Material code	Proportion of fibers (%)			Properties of nonwovens		
	1.5 denier	6 denier	15 denier	Basis weight (g/m ²)	Thickness (mm)	μ
A1	0	0	100	75	5.8	0.0097
A2	0	0	100	155	5.72	0.0196
A3	0	0	100	219	6.56	0.0242
A4	0	0	100	287	6.61	0.0315
A5	0	0	100	355	6.41	0.0401
B1	0	100	0	78	5.8	0.0097
B2	0	100	0	150	5.56	0.0195
B3	0	100	0	234	5.6	0.0303
B4	0	100	0	312	5.82	0.0388
B5	0	100	0	400	5.67	0.0511
C1	100	0	0	74	5.5	0.0097
C2	100	0	0	130	4.83	0.0195
C3	100	0	0	180	5.55	0.0235
C4	100	0	0	232	5.55	0.0303
C5	100	0	0	270	5.45	0.0359

During the preparation of these samples, the nonwoven machine and process parameters were kept constant, except the number of layers was varied during the crosslapping process. This was carried out in accordance with the desired basis weight of the materials. All of the nonwoven materials thus prepared were tested for their basis weight and thickness. The packing density values of the materials were calculated from the following formula:

$$\mu = (\lambda/T\rho_f)$$

where ρ_f was taken to be 1380 kg/m³.

Testing of nonwoven materials

The aforesaid nonwoven materials were tested for their liquid absorbent behavior with a gravimetric absorbency testing system (GATS). This system is widely used in many industries, including nonwovens, tissues, papers, textiles, clothing, apparel, powders, and polymers. This was designed to comply with ISO 9073-12 : 2002, Tappi T-561, and ASTM D 5802. It delivered liquid to the sample to be tested, recorded the weight absorbed against time, and then graphed the data. A typical setup of this system is displayed in Figure 4. It works on the principle of demand wettability. In this test, a circular sample 3.5 in. diameter was placed over a test plate, and the fluid was typically delivered to the sample through a hole of 0.25 in. in diameter situated at the bottom of the test plate from a reservoir and absorbed radially along the plane of the sample. The test plate was connected to the reservoir by means of a tube. The height of the test plate and the height of the liquid in the reservoir were kept at the same level. The height of the sample table was adjusted continuously to provide zero hydrostatic pressure. This

allowed the liquid to be taken up solely on demand by the material. The fluid reservoir was attached to a weighing balance, and the weight of the fluid transferred from the reservoir to the sample was recorded and transmitted to data acquisition software. The software plotted the weight of the liquid absorbed by the material along the ordinate and the time along the abscissa and graphed the liquid absorbency curve of the tested material. This graph was then used to estimate the capacity of absorption and the rate of absorption. The initial slope of the absorption curve divided by the dry weight of the material was taken as an estimation of the rate of absorption. The capacity of absorption was estimated as the ratio of the weight of the liquid absorbed at the terminal absorption point to the dry

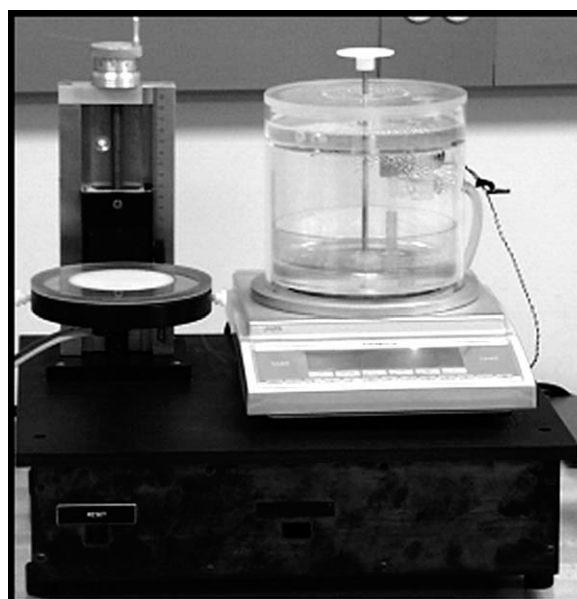


Figure 4 Image of GATS setup.

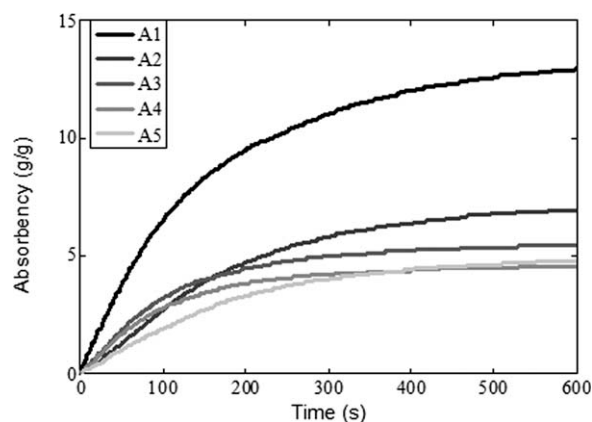


Figure 5 Plot of absorbency against time for materials A1–A5.

weight of the material. The weight of liquid absorbed was calculated by subtraction of the wet weight of the material from the dry weight of the material. In this work, distilled water was used as the test liquid.

RESULTS AND DISCUSSION

Absorption characteristics of nonwoven materials

The water absorption behaviors of the nonwoven materials made up of fibers with linear densities of 15, 6, and 1.5 denier are displayed in Figures 5, 6, and 7, respectively. Here, the time is plotted along the abscissa, and the ratio of the weight of water to the dry weight of the nonwoven material is plotted along the ordinate. It can be observed from Figure 5 that sample A1 exhibited the highest absorbency and fastest absorption among all of the nonwoven materials made up of polyester fibers 15 denier in linear density. The total absorption capacity values were observed to be 12.91 g/g for sample A1, 6.96 g/g for sample A2, 5.42 g/g for sample A3, 4.54 g/g for sample A4, and 4.78 g/g for sample A5. The rate of

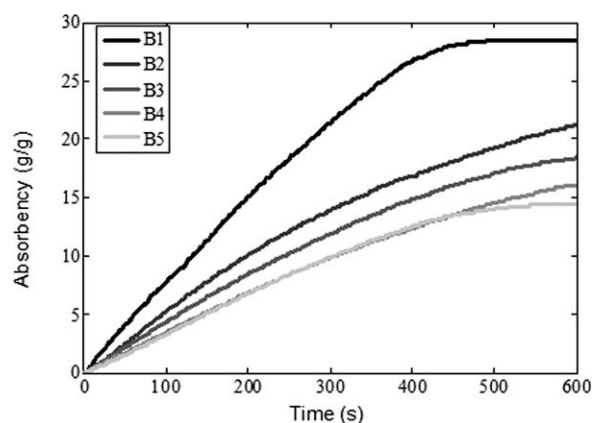


Figure 6 Plot of absorbency against time for materials B1–B5.

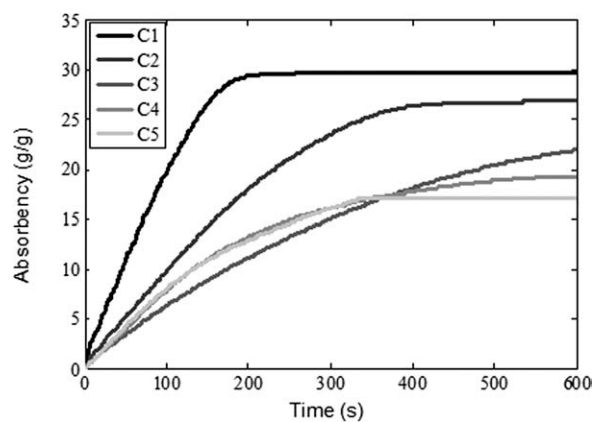


Figure 7 Plot of absorbency against time for materials C1–C5.

absorption values were found to be $0.065 \text{ g g}^{-1} \text{ s}^{-1}$ for sample A1, $0.027 \text{ g g}^{-1} \text{ s}^{-1}$ for sample A2, $0.032 \text{ g g}^{-1} \text{ s}^{-1}$ for sample A3, $0.028 \text{ g g}^{-1} \text{ s}^{-1}$ for sample A4, and $0.019 \text{ g g}^{-1} \text{ s}^{-1}$ for sample A5, respectively. Figure 6 shows that sample B1 had the highest absorbency and fastest absorption among all of the nonwoven materials made up of polyester fibers 6 denier in linear density. The total absorption capacity values were observed to be 28.55 g/g for sample B1, 21.24 g/g for sample B2, 18.45 g/g for sample B3, 16.04 g/g for sample B4, and 14.40 g/g for sample B5. The rate of absorption values were found to be $0.078 \text{ g g}^{-1} \text{ s}^{-1}$ for sample B1, $0.052 \text{ g g}^{-1} \text{ s}^{-1}$ for sample B2, $0.044 \text{ g g}^{-1} \text{ s}^{-1}$ for sample B3, $0.035 \text{ g g}^{-1} \text{ s}^{-1}$ for sample B4, and $0.033 \text{ g g}^{-1} \text{ s}^{-1}$ for sample B5. Figure 7 shows that sample C1 had the highest absorbency and fastest absorption among all of the nonwoven materials made up of polyester fibers 1.5 denier in linear density. The total absorption capacity values were observed to be 29.76 g/g for sample C1, 26.86 g/g for sample C2, 21.99 g/g for sample C3, 19.35 g/g for sample C4, and 17.11 g/g for sample C5. The rate of absorption values were found to be $0.198 \text{ g g}^{-1} \text{ s}^{-1}$ for sample C1, $0.099 \text{ g g}^{-1} \text{ s}^{-1}$ for sample C2, $0.064 \text{ g g}^{-1} \text{ s}^{-1}$ for sample C3, $0.079 \text{ g g}^{-1} \text{ s}^{-1}$ for sample C4, and $0.081 \text{ g g}^{-1} \text{ s}^{-1}$ for sample C5, respectively.

Effect of packing density on absorption characteristics

The total absorption capacity of the nonwovens made up of polyester fibers with 15, 6, and 1.5 denier linear densities are plotted against μ in Figure 8, and the rate of absorption of these nonwovens are plotted against packing density in Figure 9. The total absorption capacity and the rate of absorption of these nonwoven materials, in general, increased with decreasing μ . As expected from the model, as packing density decreased, porosity increased. Hence, more free space was available for water to

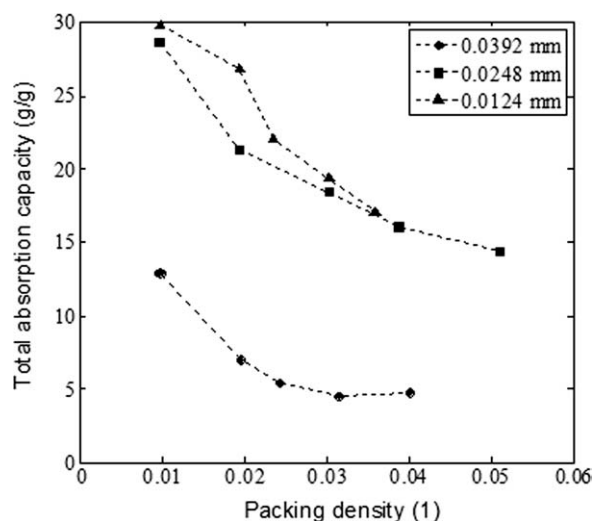


Figure 8 Plot of total absorption capacity against packing density for different fiber diameters.

enter into the structure. As a result, the absorption capacity increased with increasing porosity.

Effect of fiber diameter on absorption characteristics

The effects of fiber diameter on the total absorption capacity and the rate of absorption of the nonwovens are shown in Figures 8 and 9, respectively. It can be seen that the total absorption capacity and the rate of absorption, in general, increased with decreasing fiber diameter. As illustrated in the model reported in this article, the smaller fibers led to smaller pores, which resulted in higher capillary pressure and caused more liquid to enter into the structure relatively quickly. As a result, smaller fibers resulted in a higher absorption capacity and a higher absorption rate.

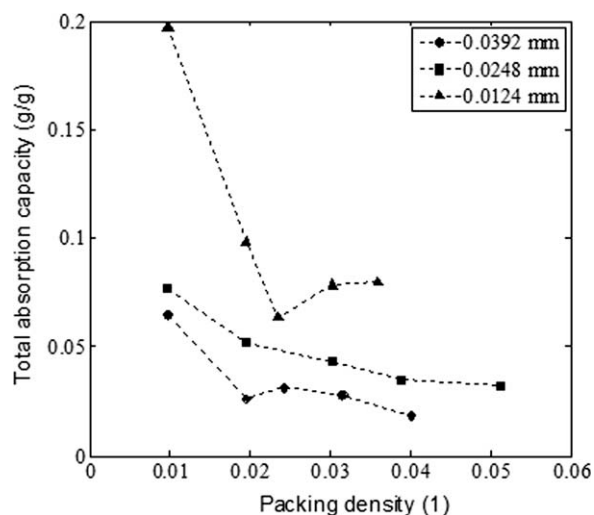


Figure 9 Plot of the rate of absorption against packing density for different fiber diameters.

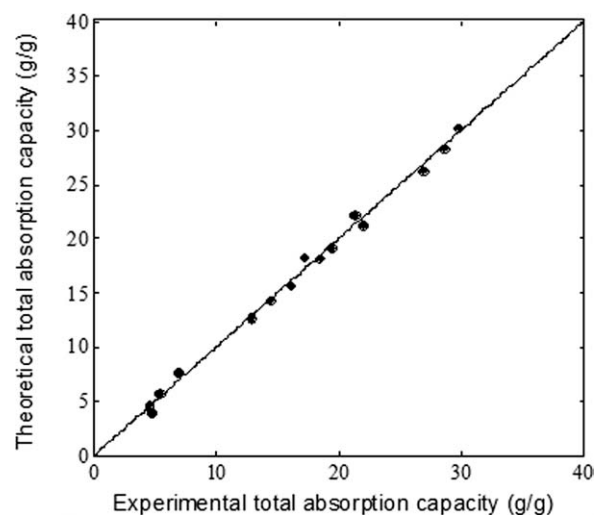


Figure 10 Plot of experimental versus theoretical total absorption capacities.

Comparison between theory and experiment

The experimental results of total absorption capacity of the nonwoven materials were compared with eq. (8), and by means of a standard nonlinear regression technique, the values of the dimensionless parameters k and m were determined. These values for the different nonwoven structures were obtained as follows: (1) $k_{[1]} = 166.67$ and $m_{[1]} = 0.2692$ for structures A1–A5, which were made up of polyester fibers 15 denier in linear density; (2) $k_{[1]} = 26.79$ and $m_{[1]} = 0.5895$ for structures B1–B5, which were made up of polyester fibers 6 denier in linear density; and (3) $k_{[1]} = 46.38$ and $m_{[1]} = 0.6183$ for structures C1–C5, which were made up of polyester fibers 1.5 denier in linear density. The theoretical total absorption capacity of the nonwovens were calculated by substitution of the values of parameters k and m in eq. (8), and these values were compared with those obtained experimentally. The results of this comparison are displayed in Figure 10. The coefficient of determination (R^2) between the theoretical results and the experimental results was found to be 0.9953. It can be thus said that the experimental results were in good agreement with the theoretical results. We observed that the value of the parameter k was the lowest and the value of the parameter m was the highest with the structure of the nonwovens made up of the finest fibers used in this study and vice versa. It is, therefore, expected that a nonwoven structure made up of finer fibers would absorb more water than a nonwoven structure made up of coarser fibers and that this difference in absorption capacity would be more prominent at lower porosities.

CONCLUSIONS

In this article, a theoretical model of the water absorption behavior of nonwoven materials is reported. This

model was verified with experimental results of polyester fibers of different cross-sectional sizes and non-woven materials of various porosities. The model was found to explain the experimental results satisfactorily. We observed that the total capacity of absorption and the rate of absorption increased with increasing porosity. The finer the fiber was, the higher the total capacity of absorption and the rate of absorption were and vice versa.

References

1. Kissa, E. *Text Res J* 1996, 66, 660.
2. Coskuntuna, E.; Fowler, A. J.; Warner, S. B. *Text Res J* 2007, 77, 256.
3. Harnett, P. R.; Mehta, P. N. *Text Res J* 1984, 54, 471.
4. Kurematsu, K.; Koishi, M. *J Colloid Interface Sci* 1984, 101, 37.
5. Zhu, L.; Perwulez, A.; Lewandowski, M.; Campagne, C. *J Appl Polym Sci* 2006, 102, 387.
6. Kawase, T.; Sekoguchi, S.; Fuj, T.; Minagawa, M. *Text Res J* 1986, 56, 409.
7. Chatterjee, P. K.; Gupta, B. S. *Absorbent Technology*; Elsevier: Amsterdam, 2002.
8. Hsieh, Y. L. *Text Res J* 1995, 65, 299.
9. Mao, N. *Text Res J* 2009, 79, 1358.
10. Dedov, A. V. *Fibre Chem* 2009, 41, 248.
11. Pan, N.; Zhong, W. *Text Prog* 2006, 38, 1.
12. Haile, W. A.; Phillips, B. M. *Tappi J* 1995, 78, 139.
13. Callegari, G.; Tyomkin, I.; Kornev, K. G.; Neimark, A. V.; Hsieh, Y. L. *J Colloid Interface Sci* 2011, 353, 290.
14. Sun, C. J.; Suen, M. C.; Chen, H. E.; Chen, C. C. *Text Res J* 2009, 79, 59.
15. Debnath, S.; Madhusoothanan, M. *J Ind Text* 2010, 39, 215.
16. Chen, X.; Vromen, P.; Lewandowski, M.; Perwuelz, A.; Zhang, Y. *Text Res J* 2009, 79, 1364.
17. Rengasamy, R. S.; Das, D.; Prabhakaran, C. *J Hazard Mater* 2011, 186, 526.
18. Gupta, B. S. *Tappi J* 1998, 71, 147.
19. Jaganathan, S.; Tafreshi, H. V.; Pourdeyhimi, B. *J Colloid Interface Sci* 2008, 326, 166.
20. Neckář, B.; Ibrahim, S. *Text Res J* 2003, 73, 611.